Traffic 2005; **6:** 1–10
Blackwell Munksgaard

doi: 10.1111/j.1600-0854.2005.00313.x

α-Latrotoxin Modulates the Secretory Machinery via Receptor-Mediated Activation of Protein Kinase C

Jie Liu[1,†], Qunfang Wan[1,†], Xianguang Lin[1], Hongliang Zhu[1], Kirill Volynski[3], Yuri Ushkaryov[3] and Tao Xu[1,2,*]

[1]*Institute of Biophysics and Biochemistry, School of Life Science and Technology, Huazhong University of Science and Technology, Wuhan 430074. P. R. China*
[2]*National Laboratory of Biomacromolecules, Institute of Biophysics, Chinese Academy of Sciences, Beijing 100101, P. R. China.*
[3]*Department of Biological Sciences, Imperial College London, London SW7 2AY, UK*
**Corresponding author: Tao Xu, xutao@ibp.ac.cn*
[†]*The authors contributed equally.*

The hypothesis whether α-latrotoxin (LTX) could directly regulate the secretory machinery was tested in pancreatic β cells using combined techniques of membrane capacitance (Cm) measurement and Ca^{2+} uncaging. Employing ramp increase in $[Ca^{2+}]_i$ to stimulate exocytosis, we found that LTX lowers the Ca^{2+} threshold required for exocytosis without affecting the size of the readily releasable pool (RRP). The burst component of exocytosis in response to step-like $[Ca^{2+}]_i$ increase generated by flash photolysis of caged Ca^{2+} was also speeded up by LTX treatment. LTX increased the maximum rate of exocytosis compared with control responses with similar postflash $[Ca^{2+}]_i$ and shifted the Ca^{2+} dependence of the exocytotic machinery toward lower Ca^{2+} concentrations. LTX^{N4C}, a LTX mutant which cannot form membrane pores or penetrate through the plasma membrane but has similar affinity for the receptors as the wild-type LTX, mimicked the effect of LTX. Moreover, the effects of both LTX and LTX^{N4C} were independent of intracellular or extracellular Ca^{2+} but required extracellular Mg^{2+}. Our data propose that LTX, by binding to the membrane receptors, sensitizes the fusion machinery to Ca^{2+} and, hence, may permit release at low $[Ca^{2+}]_i$ level. This sensitization is mediated by activation of protein kinase C.

Key words: calcium, exocytosis, insulin, latrophilin, PKC, α-latrotoxin

Received 3 April 2005, revised and accepted for publication 23 May 2005, published on-line XXXX

The black-widow spider neurotoxin α-latrotoxin (LTX) causes massive stimulation of neurotransmitter release by exocytosis after binding to specific high-affinity membrane receptors (1,2). Several structurally and functionally unrelated membrane receptors for LTX have been proposed. The first receptor discovered was neurexin (3,4), which binds LTX only in the presence of Ca^{2+}. As LTX was known to act in the absence of Ca^{2+}, this led to the eventual discovery of a Ca^{2+}-independent receptor for LTX (CIRL); or latrophilin (5,6). Latrophilin is a seven-transmembrane protein that belongs to the secretin/calcitonin family of G protein-coupled receptors (7,8). Recently, a third receptor for LTX, protein tyrosine phosphatase σ (PTPσ), has been described that binds toxin in a Ca^{2+}-independent manner (9). However, the fact that LTX exhibited only minor residual activity in the neurexin and latrophilin double knockout mice suggests that PTPσ might represent a minor receptor for LTX (10).

The mechanism of action of LTX has been elusive. LTX has long been known to form Ca^{2+}-permeable non-selective pores in the plasma membrane (11). LTX forms dimers in solution that may assemble further into tetramers or higher order oligomers in the presence of divalent cations; the tetramers can insert themselves into the membrane (12). However, when triggering exocytosis, the toxin does not simply act as an ionophore for Ca^{2+}. Evidence is accumulating that LTX is still active in the absence of extracellular Ca^{2+} (13,14), suggesting an additional, Ca^{2+}-independent mechanism. It is generally believed that the major Ca^{2+}-dependent effect is due to the Ca^{2+} entry through the toxin pore, whereas the Ca^{2+}-independent effect results from receptor-mediated signaling. The binding of the toxin to latrophilin has been proposed to induce IP_3 generation via activation of phospholipase C (PLC) and stimulate release of Ca^{2+} from intracellular stores (15). It has been proposed that the mobilization of intracellular Ca^{2+} plays a pivotal role in mediating the effect of the toxin (15,16). However, this transduction pathway actually requires extracellular Ca^{2+} (16,17), and it is argued that the Ca^{2+}-independent effect of LTX cannot be due to signaling from latrophilin to Ca^{2+} stores (for review see 18). Instead, it has been proposed that the vesicular exocytosis triggered by LTX in the absence of Ca^{2+} might be due to its membrane penetration and/or pore formation. It is unclear whether the membrane penetration of the toxin could directly modulate the secretory machinery and, hence, trigger exocytosis, as hypothesized recently (19).

The general exocytotic machinery seems to be conserved in exocytosis of large dense core vesicles (LDCVs) in endocrine cells (20–22) and synaptic vesicles in neuronal cells. LTX has also been shown to be effective in mediating Ca^{2+}-independent exocytosis of LDCVs from pancreatic β cells (23), pituitary gonadotropes (24) and chromaffin cells (25). Elucidation of the mechanism of LTX action will probably lead to significant insights into how exocytosis is controlled. In the current study, we explore the

mechanism of the Ca^{2+}-independent action of LTX on exocytosis in primarily cultured pancreatic β cells and test the hypothesis whether LTX could directly regulate the secretory machinery. Using combined techniques of membrane capacitance (Cm) measurement and Ca^{2+} uncaging, we show that LTX accelerates the fusion kinetics of the readily releasable pool of vesicles (RRP), and this modulation of the release machinery does not require extracellular Ca^{2+}. The effect is mimicked by a LTX mutant, LTX^{N4C}, which cannot form membrane pores and interact with the fusion machinery (26,27), indicating that the toxin sensitizes exocytosis to Ca^{2+} indirectly, by activating a receptor-mediated mechanism.

Results

LTX induces Ca^{2+} influx via pore formation

In standard bath solution containing 2.6 mM Ca^{2+}, application of LTX triggered significant $[Ca^{2+}]_i$ elevation in rat pancreatic β cells as assayed by the fluorescence ratio of fura-2 excited at 340 and 380 nm. Figure 1A shows four typical responses induced by different concentrations of LTX (10 pM, 100 pM, 500 pM and 3 nM). It is evident that the effect of LTX on $\Delta[Ca^{2+}]_i$ elevation is dose dependent. Figure 1B plots the increment in $[Ca^{2+}]_i$ ($\Delta[Ca^{2+}]_i$) as a function of the concentration of LTX. The EC_{50} of LTX on $[Ca^{2+}]_i$ in β cells was estimated to be 0.16 nM, and the maximum effect was achieved at 3 nM. In the following experiments, we thus employed LTX at a concentration of 3 nM to test its effect on exocytosis.

To verify the source of $[Ca^{2+}]_i$ elevation induced by LTX, we monitored the whole-cell membrane current and $[Ca^{2+}]_i$ simultaneously from voltage-clamped (holding potential −70 mV) β cells. We observed flickering of inward current accompanied by concurrent changes in $[Ca^{2+}]_i$ (data not shown), which is consistent with the pore-forming capability of LTX. To estimate the unitary conductance, we measured the amplitude of unitary LTX-induced current from individual cells that were held at potentials of −40, −70 and −100 mV. Three typical examples of current records at different clamped voltages are shown in Figure 2A. Figure 2B plots the unitary current amplitude as a function of the membrane potential. These data suggest that the LTX-induced current in β cells has a unitary conductance of 0.13 nS in our bath solution, and the current reverses at −4.8 mV. To further test whether the extracellular Ca^{2+} is necessary for the $[Ca^{2+}]_i$ elevation induced by LTX, we compared the $[Ca^{2+}]_i$ elevation induced by LTX in the presence and absence of extracellular Ca^{2+}. As shown in Figure 2C, in standard bath solution, LTX elevated $[Ca^{2+}]_i$ from 85 ± 8 nM to a mean peak value of 445 ± 44 nM, whereas in Ca^{2+}-free bath solution, no significant $[Ca^{2+}]_i$ elevation could be induced by LTX. These results suggest that LTX induced $[Ca^{2+}]_i$ rise in pancreatic β cells via formation of Ca^{2+}-permeable pores, as previously suggested (11,24).

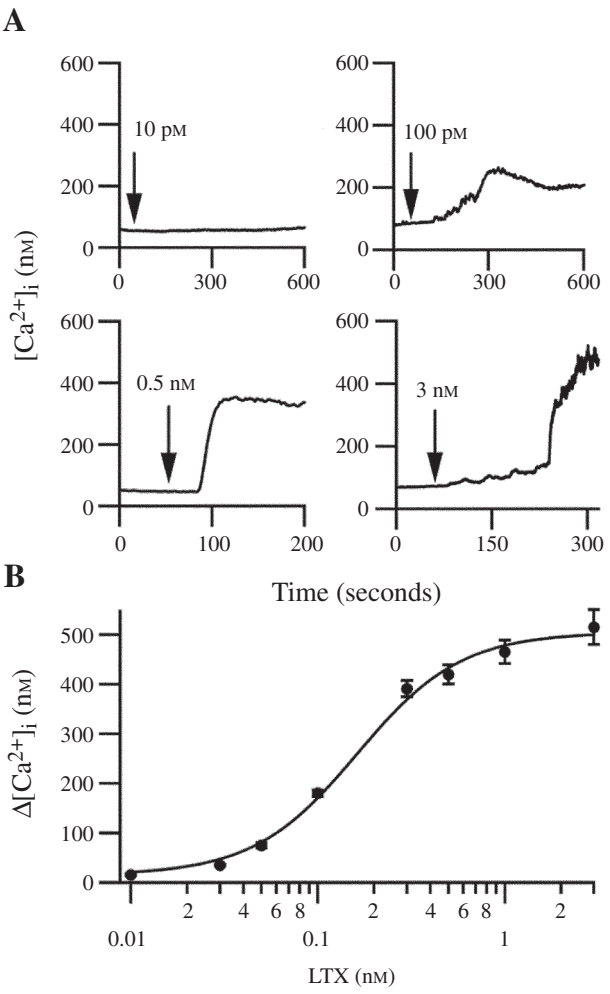

Figure 1: LTX induces $[Ca^{2+}]_i$ elevation in the presence of extracellular Ca^{2+}. A) Four examples of LTX's effect on $[Ca^{2+}]_i$ at indicated toxin concentrations. $[Ca^{2+}]_i$ was assayed by the ratio of fura-2 fluorescence with alternating excitation at 340 and 380 nm. Note that as the concentration of LTX increases, so does the increment in $[Ca^{2+}]_i$. LTX was perfused throughout the experiment starting from the times indicated by arrows. B) Dose dependence of LTX's effect on the $[Ca^{2+}]_i$ increase ($\Delta[Ca^{2+}]_i$). Data were averaged from five to nine cells. The maximal effect of LTX is achieved at 3 nM.

LTX lowers the Ca^{2+} threshold required for exocytosis

To avoid the drastic effect of Ca^{2+} influx through the LTX pores, we performed the following experiments in bath solution containing 1 mM EGTA and 1.2 mM Mg^{2+} with no added Ca^{2+}. Identifying mechanisms of LTX effects on exocytosis is complicated by the range of possible targets that may contribute in concert. In the present study, we simplified the task by photoreleasing intracellular Ca^{2+} from a caged Ca^{2+} compound [DM-nitrophen (DMN)] as the stimulus. Using Cm as a measure of exocytosis and simultaneously monitoring $[Ca^{2+}]_i$ changes generated by Ca^{2+} uncaging, we could test the influence of LTX on the fusion apparatus. We first employed the ramp $[Ca^{2+}]_i$ stimulation generated by continuous UV

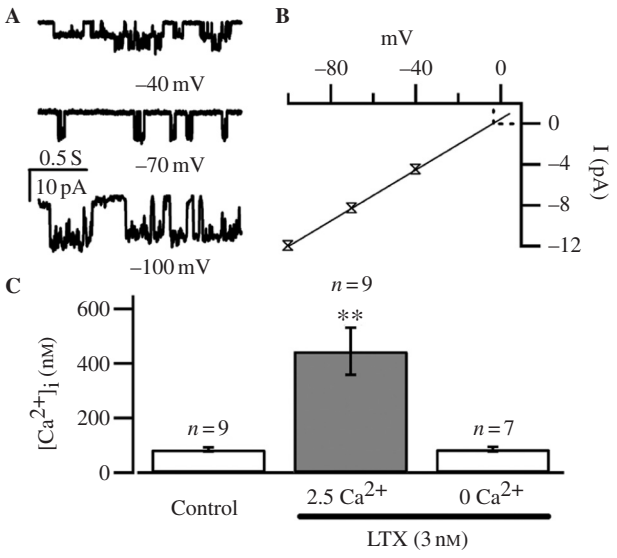

Figure 2: LTX induces Ca^{2+} influx via pore formation in the presence of extracellular Ca^{2+}. A) LTX-induced channel currents were recorded in the whole-cell patch-clamp mode during the initial phase of pore formation. Example traces at three different pipette potentials (−40, −70 and −100 mV) are displayed. The input resistance under the recording conditions ranged from 1 to 2 GΩ. B) Current-voltage relation of the LTX-induced unitary current. The data points at different pipette potentials were mean values of the unitary amplitude of LTX-induced current obtained from four cells. The dotted line is a linear fit with a slope of 0.13 nS and an X-intercept of −4.8 mV. C) Summary of the peak $[Ca^{2+}]_i$ before and after LTX (3 nM) treatment in the presence and absence of extracellular Ca^{2+}. LTX-induced $[Ca^{2+}]_i$ elevation is abolished after removal of extracellular Ca^{2+}.**Significant difference ($p < 0.01$, *t*-test) compared with control condition.

illumination. As shown in Figure 3A, the steady UV illumination released Ca^{2+} from caged Ca^{2+} continuously, increasing $[Ca^{2+}]_i$ gradually by several μM within seconds. The plasma membrane area (recorded as Cm) remained constant at the beginning when $[Ca^{2+}]_i$ was low but at a certain point took off rapidly. Then with depletion of the RRP, the change of Cm slowed down. To quantify the effects of LTX, we took the $[Ca^{2+}]_i$ level at the half-maximal rate of exocytosis ($[Ca^{2+}]$Rmax/2) as our index of the $[Ca^{2+}]_i$ sensitivity of exocytosis. To estimate the RRP size, we fitted a straight line to the last slow phase of the Cm increase and extrapolated it back to the time when the half-maximal rate was reached. The calculated difference (ΔCm) between this extrapolated level and the baseline Cm was our measure of RRP size. As shown in Figure 3B, LTX did not significantly increase the RRP size measured this way (control, 221 ± 14 fF; LTX, 251 ± 30 fF). In contrast, LTX reduced the $[Ca^{2+}]R_{max}/2$ for exocytosis from 2.9 ± 0.3 μM in control cells to 1.1 ± 0.3 μM in cells treated with LTX (Figure 3C), suggesting that LTX increases the Ca^{2+} sensitivity of exocytosis.

LTX accelerates the kinetics of the exocytotic burst

To validate conclusions drawn from our $[Ca^{2+}]_i$ ramp experiments, we used flash photolysis of caged Ca^{2+} to raise $[Ca^{2+}]_i$ in a step-like manner. The $[Ca^{2+}]_i$ step elicits a burst of exocytosis followed by a slow continuous component as previously demonstrated (28,29). To compare the kinetics of exocytosis at similar $[Ca^{2+}]_i$ levels, we averaged the burst components from experiments with similar postflash $[Ca^{2+}]_i$ values (measured 20 ms after the flash) between 2 and 3 μM (mean $[Ca^{2+}]_i$ values were control, 2.8 ± 0.03 μM, $n = 4$; LTX, 2.7 ± 0.1 μM, $n = 6$). As shown in Figure 4A, LTX treatment speeds up the burst component. We fitted the averaged burst component with single exponentials and obtained rate constants of 5/second and 18/second for control and LTX-treated groups, respectively. We also analyzed the maximum rate of exocytosis from individual responses with postflash $[Ca^{2+}]_i$ between 3 and 4 μM. The maximum rate of exocytosis was estimated by dividing the increment of Cm at time τ/2 by $\Delta t = \tau/2$, where τ is the time constant from the exponential fit of the burst component. As shown in Figure 4C, LTX increased the maximum rate of exocytosis from 762 ± 117 fF/second ($n = 16$) in control cells to 1621 ± 257 fF/second ($n = 15$). The corresponding mean $[Ca^{2+}]_i$ levels were 3.5 ± 0.1 and 3.6 ± 0.1 μM for control and LTX-treated cells, respectively. In contrast, the RRP size was not vastly affected by LTX (Figure 4B).

We further plotted the rate constants for exponential fits of exocytotic bursts against postflash $[Ca^{2+}]_i$ levels for control and LTX-treated cells, which gives the Ca^{2+} dependence of the RRP fusion. As shown in Figure 5, LTX shifts the Ca^{2+} dependence towards lower Ca^{2+} concentrations, confirming the conclusion from the Ca^{2+} ramping experiments above that LTX sensitizes the exocytosis of the RRP to Ca^{2+}. Every point in the Figure 5 denotes the averaged rate constants, and $[Ca^{2+}]_i$ levels of 4–6 points derived from individual responses with similar $[Ca^{2+}]_i$.

Abolition of the LTX effect on exocytosis in the absence of both Ca^{2+} and Mg^{2+}

LTX triggers exocytosis only after binding to its membrane receptors. Divalent cations such as Ca^{2+} and Mg^{2+} have been demonstrated to be important for the function of LTX. It has been shown that neurexin binds LTX only in the presence of Ca^{2+} (30,31) and therefore cannot participate in the toxin action described above. Surprisingly, the Ca^{2+}-independent receptor for LTX, latrophilin, also seems to critically require extracellular Ca^{2+} to mediate exocytosis stimulation by LTX. On the other hand, in the absence of Ca^{2+}, Mg^{2+} has been shown to facilitate toxin tetramerization and pore formation. Mg^{2+} is also required for LTX-stimulated release in Ca^{2+}-free conditions (32). To test whether the above effect of LTX on the kinetics of exocytosis required Mg^{2+} in the absence of Ca^{2+}, we repeated the same experiment in the bath solution in the absence of both Ca^{2+} and Mg^{2+}. We found that the effect of LTX was abolished when both Ca^{2+} and Mg^{2+} were omitted from the bath solution in the presence of 1 mM EGTA. As shown in Figure 6A, the averaged burst components exhibit indistinguishable kinetics between control

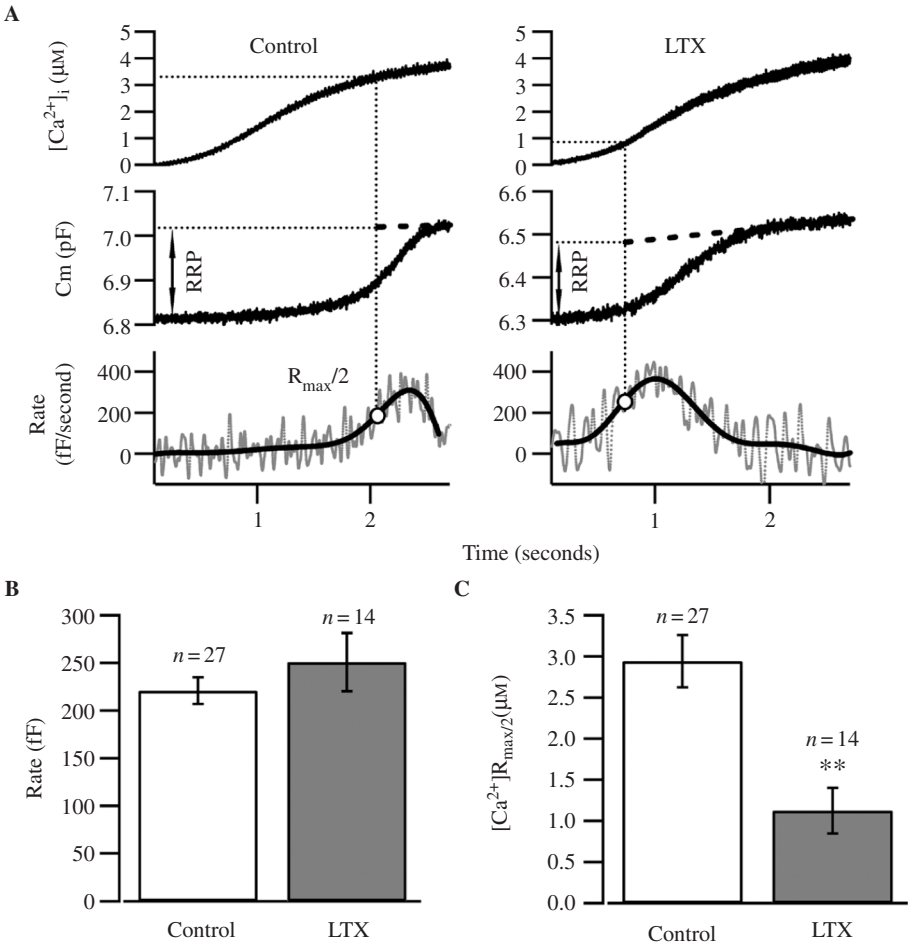

Figure 3: LTX lowers the Ca^{2+} threshold for exocytosis. A) Steady UV illumination generates ramp $[Ca^{2+}]_i$ increases with intracellular caged Ca^{2+} and measures $[Ca^{2+}]_i$ by using a Ca^{2+} indicator, fura-6F. Simultaneous time courses of $[Ca^{2+}]_i$, membrane capacitance (Cm) and the rate of exocytosis for a single control β cell (left) and for a LTX-treated β cell (right). The rate of exocytosis was derived from the derivative of Cm trace (gray noisy trace) and fitted with a polynomial function (smooth line), from which we measure the $[Ca^{2+}]_i$ level at the half-maximal rate ($[Ca^{2+}]R_{max}/2$). The vertical dotted lines indicate the time when the half-maximal exocytosis rate is reached. We fitted a straight line (dashed line) to the last slow phase of the Cm increase and extrapolated it back to the time when the half-maximal rate was reached. The difference (ΔCm) between this extrapolated level and the baseline Cm was our measure of RRP size. B) LTX exerts no significant effect on the RRP size. C) LTX significantly reduces the calcium threshold (measured as $[Ca^{2+}]$ $R_{max}/2$) for exocytosis. **Significant difference ($p < 0.01$, *t*-test) compared with control condition.

and LTX-treated cells. The mean RRP size and the maximum rate of exocytosis are also unchanged by LTX (Figure 6B,C). This result demonstrates that the action of LTX on the fusion machinery actually needs extracellular divalent cations.

LTX^{N4C} accelerates the kinetics of the exocytotic burst

It is usually very difficult to study any intracellular reactions of LTX in the presence of the toxin pores, whose effect might be much stronger. To avoid this complication and also to distinguish any possible direct interaction of LTX with the release machinery from its receptor-mediated actions, we have taken the advantage of the recently developed mutant toxin, LTX^{N4C}. LTX^{N4C} binds to the receptor with similar affinity as the wild-type toxin, but neither forms pores nor penetrates through the plasma membrane (17,26,27).

We performed the same experiments as done with wild-type LTX to assess the effect of LTX^{N4C} on exocytosis. The Cm responses to similar $[Ca^{2+}]_i$ steps were averaged for control and LTX^{N4C}-treated cells. As displayed in Figure 7A, LTX^{N4C} accelerates the kinetics of the averaged exocytotic burst. With similar mean $[Ca^{2+}]_i$ values of 2.8 ± 0.03 ($n = 4$) and 2.7 ± 0.05 μM ($n = 9$) for control and LTX^{N4C}-treated cells, respectively; the rate constant of exponential fit to the burst component was increased from 5/second to 16/second by LTX^{N4C} treatment. LTX^{N4C} also shifted the Ca^{2+} dependence of the rate constants toward lower Ca^{2+} concentrations, as shown in Figure 7B. In addition, LTX^{N4C} increased the maximum

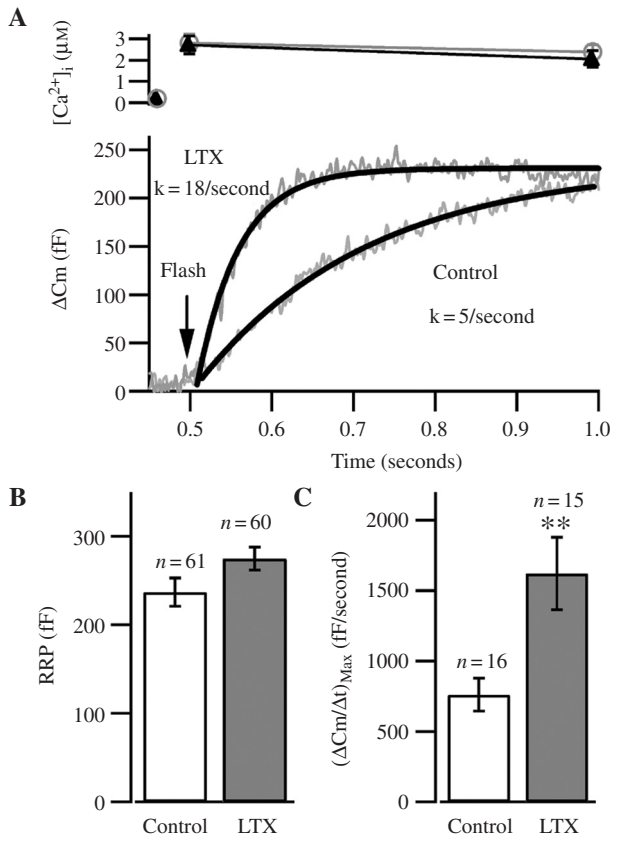

Figure 4: LTX accelerates the kinetics of the exocytotic burst. A) Averaged $[Ca^{2+}]_i$ and membrane capacitance (Cm) changes (ΔCm) for Control and LTX-treated cells (3 nM), summarizing experiments that had postflash $[Ca^{2+}]_i$ values between 2 and 3 μM. Superimposed curves are single exponential fits with the rate constants indicated. B) RRP size is not significantly changed by LTX pretreatment. C) LTX increases the maximum rate of exocytosis. The maximal rate of exocytosis is obtained by dividing the change of capacitance (ΔCm) at time τ/2 by $\Delta t = \tau/2$, where τ is the time constant from the exponential fit of the exocytotic burst.

rate of exocytosis compared with control responses with similar postflash $[Ca^{2+}]_i$ (Figure 7D), without significantly affecting the RRP size (Figure 7C).

Sensitization of the secretory machinery by LTX involves activation of protein kinase C

Activation of latrophilin by LTX has been suggested to stimulate the production of IP_3 and diacylglycerol (DAG). DAG is known to activate protein kinase C (PKC) as well as Munc13 (33,34). To determine which of these pathways is involved in the stimulatory effect of LTX, we included 1 μM Gö6983, a specific inhibitor of PKC, in the patch pipette and performed the exocytosis assay stimulated by ramp $[Ca^{2+}]_i$ increase. The reason to use ramp $[Ca^{2+}]_i$ stimulation is that both the RRP size and the Ca^{2+} threshold for exocytosis can be estimated simultaneously during stimulation of a single cell. As shown in Figure 8, intracellular

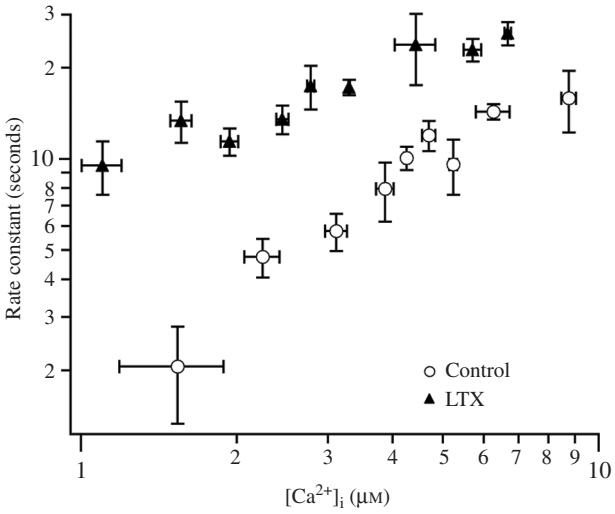

Figure 5: LTX increases the Ca^{2+} sensitivity of release. The rate constants of exponential fits to the exocytotic bursts with similar postflash $[Ca^{2+}]_i$ levels are averaged and plotted versus $[Ca^{2+}]_i$ levels for control (circles) and LTX-treated (filled triangles, 3 nM for 2–3 min) pancreatic β cells. Every point represents the averaged rate constant and $[Ca^{2+}]_i$ levels of 4–6 points derived from individual responses with similar $[Ca^{2+}]_i$.

dialysis of Gö6983 blocked the effect of either LTX or LTX^{N4C} in lowering the Ca^{2+} threshold for exocytosis. PKC19-31, a pseudosubstrate peptide that interacts with the PKC substrate binding site in the catalytic domain, also abolished the effect of LTX when included (1 μM) in the pipette solution (data not shown). These results suggest that PKC activation is required for the receptor-mediated modulation of the secretory machinery by LTX.

Discussion

As LTX affects the release of all types of neurotransmitters (35) as well as hormones, it is likely to target an essential and ubiquitous component of the secretory machinery. Hence, the mechanism of action of the toxin has been intensively investigated (for review see 36). Multiple mechanisms of action have been suggested for LTX, but has been difficult to elucidate the exact mechanism underlying the action of LTX under specific conditions. The main problem is the complex mode of action of LTX, which may also vary between the different systems used to study exocytosis. First of all, the toxin binds to receptors and could activate them. Then LTX inserts itself into the plasma membrane and forms stable non-selective cation channels (37–39). The influx of Ca^{2+} through the cation channels causes massive Ca^{2+}-dependent exocytosis (11). Because the toxin partially penetrates the cell membrane, it might also directly affect the exocytotic apparatus. The aim of this study was to investigate the receptor-mediated effect versus direct modulation on secretory machinery by LTX.

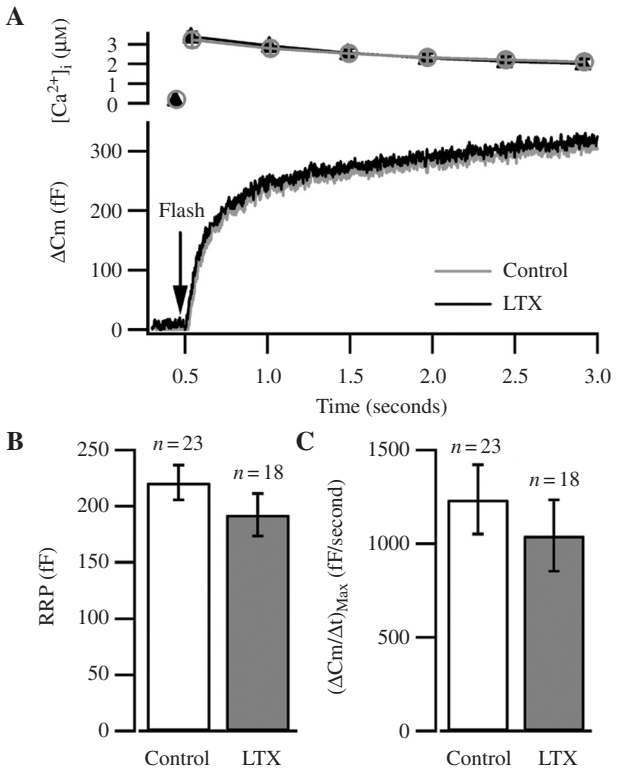

Figure 6: Abolition of the LTX effect on exocytosis in the absence of both Ca^{2+} and Mg^{2+}. A) In the absence of both Ca^{2+} and Mg^{2+}, LTX (3 nM) does not affect the time–course of the burst component. Averaged burst components with postflash $[Ca^{2+}]_i$ values between 3 and 5 μM from Control and LTX-treated cells are displayed for comparison. Arrow indicates the time where flash was triggered. B) RRP size is not significantly changed by LTX pretreatment. C) LTX fails to increase the maximum rate of exocytosis in the absence of both Ca^{2+} and Mg^{2+}.

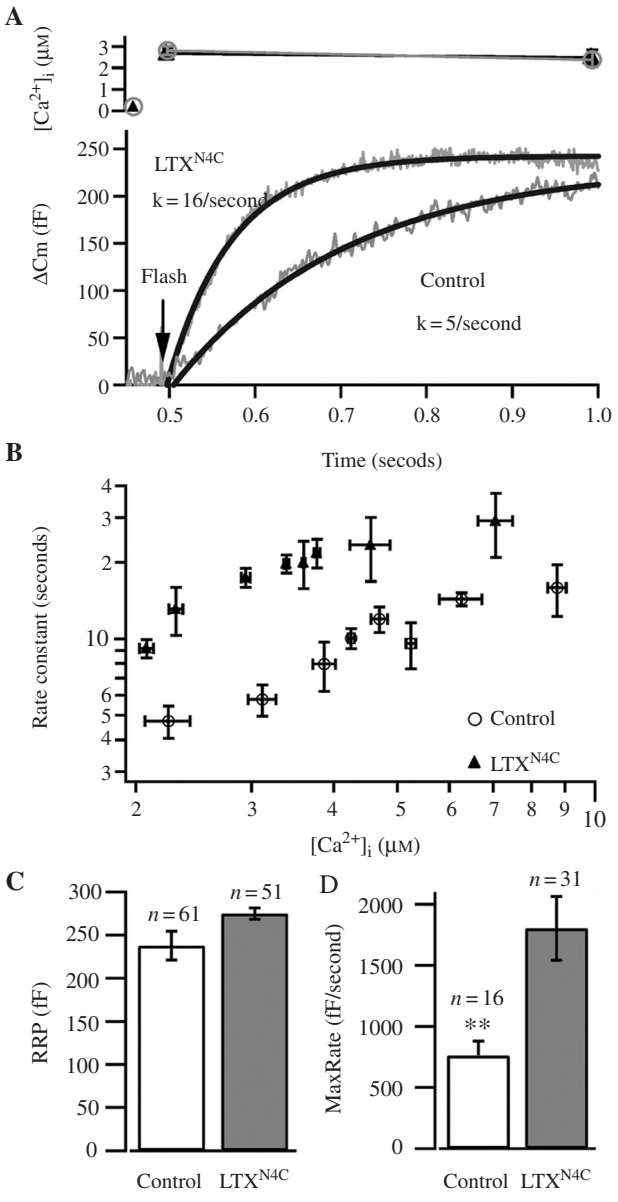

Figure 7: LTX^{N4C} accelerates the kinetics of the exocytotic burst. A) Averaged $[Ca^{2+}]_i$ and membrane capacitance changes (ΔCm) for Control and LTX^{N4C}-treated cells (3 nM), summarizing experiments that had postflash $[Ca^{2+}]_i$ values between 2 and 3 μM. Superimposed curves are single exponential fits with the rate constants indicated. B) Rate constants for exponential fits to the exocytotic burst with similar postflash $[Ca^{2+}]_i$ levels are averaged and plotted versus $[Ca^{2+}]_i$ levels for control (circles) and LTX^{N4C}-treated (filled triangles, 3 nM for 2–3 min) pancreatic β cells. C) RRP size is not significantly changed by LTX^{N4C} pretreatment. D) LTX^{N4C} increases the maximum rate of exocytosis.**Significant difference ($p < 0.01$, *t*-test) compared with control condition.

However, it is very hard to study any receptor signaling or direct interaction with secretory machinery in the presence of the toxin pores, whose effect is usually much stronger. Therefore, it is very important to design experiments to separate the receptor- and pore-mediated effects of LTX. Although the pore can be blocked by trivalent ions, they often block the Ca^{2+} channels and do not allow investigating the Ca^{2+}-evoked exocytosis. In this study, we have blocked the Ca^{2+} influx through the pores by incubating the cells in nominally Ca^{2+}-free bath solution. Exocytosis was evoked by photorelease of Ca^{2+} via photolysis of caged Ca^{2+}. The advantage of the photolysis technique is that it generates well-controlled homogeneous elevation of intracellular Ca^{2+} concentration, which avoids the complication of pore-mediated Ca^{2+} influx or the modulation of the Ca^{2+} signaling by LTX. Thus, the effects of LTX on secretory machinery can be directly assessed. LTX has also been postulated to cause efflux of neurotransmitters through toxin pores (15,17,40), which further complicated the interpretation of the stimulatory effect of LTX. However, this mechanism will not be reflected in the current study, because we employed the Cm measurement to monitor the membrane surface change caused by fusion of secretory vesicles. To further ascertain the role of receptor signaling, we have utilized a mutant toxin, termed LTX^{N4C}, which contains a small insert

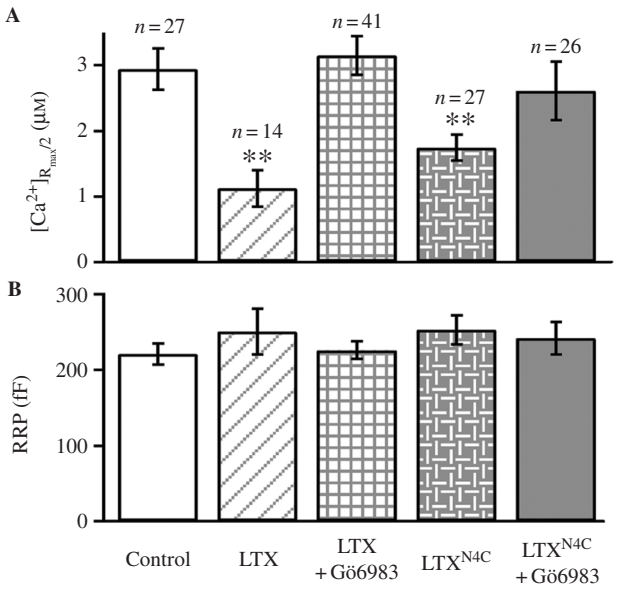

Figure 8: The effect of LTX is mediated by activation of protein kinase C (PKC). Ramp $[Ca^{2+}]_i$ increases were generated to estimate the RRP size and the Ca^{2+} threshold (measured as $[Ca^{2+}]R_{max}/2$) for exocytosis as done in Figure 4. Summary of the effects of different treatments on the $[Ca^{2+}]R_{max}/2$ (A) and RRP size (B). The lowering of the Ca^{2+} threshold for exocytosis by either LTX or LTX^{N4C} was blocked by a specific PKC inhibitor, Gö6983. **Significant difference ($p < 0.01$, *t*-test) compared with control condition.

within the domain responsible for the formation of the ring-like tetramers (12). As a result, LTX^{N4C} is unable to form pores but retains the ability to induce receptor signaling and cause massive release in several secretory systems (16,27). This mutant has an additional advantage that it cannot directly interact with the exocytotic apparatus.

Through a combination of the methods of Ca^{2+} uncaging and Cm measurement, as well as the blockade of Ca^{2+} influx and the use of LTX^{N4C}, we have restricted our analysis to the effect of receptor-mediated signaling on exocytosis. Latrophilin has been implicated as the main signaling receptor for LTX and LTX^{N4C}. Latrophilin is a G protein-coupled receptor thought to be linked to Gαq/11 (41). The downstream effector of Gαq/11 is PLC. LTX-activated PLC stimulates hydrolysis of phosphoinositides and increases the cytosolic concentration of IP_3 (26). IP_3 in turn induces release of Ca^{2+} from the intracellular stores. It has been suggested that mobilization of intracellular Ca^{2+} appears to play a pivotal role in mediating the stimulatory effect of LTX. LTX^{N4C} has been demonstrated to increase the rate of spontaneous exocytosis and the amplitude of evoked release (16). This effect can be abolished by both inhibiting IP_3-induced Ca^{2+} release and by depleting Ca^{2+} stores with thapsigargin (16,17). Chelation of cytosolic Ca^{2+} by membrane permeable BAPTA-AM also blocks the LTX^{N4C} action. Finally, LTX^{N4C} was directly shown to induce a rise in the presynaptic $[Ca^{2+}]_i$ (16). However, in the current study, intracellular Ca^{2+} stores probably play a less prominent role in the sensitization of the release machinery, because caged Ca^{2+} used in the flash experiments would act as a strong, although slow, Ca^{2+} chelator to buffer Ca^{2+} fluctuations. Moreover, we have shown that LTX fails to generate any obvious Ca^{2+} signal in the absence of extracellular Ca^{2+}. Similar results have been obtained previously indicating that LTX cannot induce $[Ca^{2+}]_i$ elevation in Ca^{2+}-free solution in INS-1 cells and pituitary gonadotropes (23,24). These results suggest that a mechanism other than Ca^{2+} mobilization might also participate in mediating the stimulatory effect of LTX on exocytosis.

LTX has been shown to trigger exocytosis even in the absence of extracellular Ca^{2+} and when the intracellular Ca^{2+} is strongly buffered (24). The mechanism underlying the Ca^{2+}-independent action of LTX remains to be established. Using protection from proteolysis, it has been suggested that the insertion of LTX into the plasma membrane after receptor binding results in protection of the N-terminal sequences (19). It was postulated that the internalized N-terminal part of the toxin could exert a direct fusogenic effect on the secretory machinery. While this hypothesis sounds fascinating, there is virtually no evidence to support a direct modulation of the secretory machinery by LTX. It is believed that the identification of the molecular targets for LTX would lead to significant insight into how exocytosis is mediated.

In the current study, we have been able to check, for the first time, whether LTX affects the kinetics of the fusion event in pancreatic β cells. Upon step-like $[Ca^{2+}]_i$ elevation by flash photolysis, exocytosis proceeds with an initial, rapid exocytotic burst followed by a slower, sustained phase. The initial burst component is believed to represent the fusion of the readily releasable vesicles. The kinetics of the burst component may, thus, reflect the processes of Ca^{2+} binding and unbinding to the so-called Ca^{2+} sensor and the final fusion. We have shown that LTX accelerates the kinetics of the exocytotic burst, suggesting that LTX might affect the fusion machinery to increase its Ca^{2+} sensitivity. This idea is further supported by our Ca^{2+} ramp experiment, where we showed that the $[Ca^{2+}]_i$ threshold required for exocytosis is lowered by LTX treatment.

It is, thus, plausible that LTX might transform the readily releasable vesicles into a highly Ca^{2+}-sensitive state by interacting directly or indirectly with the fusion machinery. The internalized part of the toxin might mediate a direct interaction. However, by using the mutant toxin, we demonstrate unequivocally that the effect of LTX is mediated by an indirect signaling pathway generated upon binding of the toxin to its membrane receptor. It should be noted that while PLC activation downstream of latrophilin stimulates the production of IP_3, it also produces DAG. DAG has been known as an endogenous

activator of PKC as well as Munc13 (33,34). By employing a specific inhibitor of PKC (Gö6983), which does not block the function of Munc13, we have shown that the sensitization of the secretory machinery is mediated by PKC activation. This is consistent with a recent finding that PKC activation stimulates the appearance of a highly calcium sensitive pool (HCSP) of vesicles in β cells (29,42). Indeed, the kinetics of fusion after LTX treatment closely resembles that of HCSP.

In a previous study, a role of PKC has been implicated in the action of LTX in permeabilized chromaffin cells (43). However, the study proposed that PKC activation is not due to receptor-mediated activation of PLC pathway, but rather requires high micromolar Ca^{2+} that directly enters permeabilized cells. Hence, the previous data do not support a receptor-mediated signaling pathway but rather propose a secondary activation of PKC through Ca^{2+} entry from the LTX pore (43). It remains to be established whether the receptor-mediated signaling pathway exists in intact cells, which may reflect the physiological function of the still unknown endogenous ligand for latrophilin. Moreover, it remains to be established how the receptor-mediated signaling pathway affects exocytosis in intact cells. Our results suggest a receptor-mediated activation of PKC by latrophilin and subsequent sensitization of the secretory machinery. Given the third-power to fourth-power dependence of exocytosis on intracellular free Ca^{2+} concentration, even a small change in the Ca^{2+} sensitivity could have large effects on the overall exocytotic rate. Extrapolation of the graph in Figure 5 indicates that the release rate may be increased even at the resting Ca^{2+} level (100 nM). It must be pointed out, however, that the rate of release under these conditions would be too low (less than 1 event/second) to be detected in our experiments, because slow increases in Cm would be compensated by endocytosis. Hence, sensitization of the fusion machinery to Ca^{2+} provides an explanation for the long-recognized Ca^{2+}-independent stimulation on exocytosis by LTX from intact cells, to permit release at low $[Ca^{2+}]_i$.

Materials and Methods

Materials

LTX was purchased from Alomone Laboratories (Jerusalem, Israel). Gö6983 was purchased from Calbiochem (La Jolla, CA, USA). Procedures for LTX^{N4C} expression and isolation were described previously (27). Briefly, LTX^{N4C} was purified from the baculovirus expression medium by affinity chromatography on immobilized anti-LTX mAb (A-15), dialyzed and concentrated to approximately 40 nM.

Cell culture

Pancreatic β cells from adult male Wistar rats were prepared and cultured as described previously (44). Briefly, pancreatic islets were isolated by collagenase digestion of the pancreas from male Wistar rats. The islets were further digested by dispase II to dissociate single β cells. The dispersed β cells were plated on glass coverslips and kept in DMEM (Gibco, Grand Island, NY, USA) supplemented with 10% (v/v) fetal calf serum (Gibco), 100 μg/mL of penicillin and 100 mg/mL of streptomycin (Gibco). The normal bath solution for experiments contained 138 mM NaCl, 5.6 mM KCl, 1.2 mM $MgCl_2$, 2.6 mM $CaCl_2$, 5 mM D-glucose and 10 mM HEPES (pH 7.4 adjusted with NaOH). The Ca^{2+} free external bath solution consisted of similar components, except $CaCl_2$ was substituted for 1 mM EGTA. All experiments were performed at 32–33 °C on cells with diameter of 11–12 μm. Conservatively, these cells had a >80–90% probability of being β cells (45). Sometimes, we have verified our selection by the presence of K_{ATP} channels and by the $[Ca^{2+}]_i$ responses to glucose.

Ca^{2+} uncaging and $[Ca^{2+}]_i$ measurement

$[Ca^{2+}]_i$ was measured by dual-wavelength excitation (340/380 nm) microfluorometry using either fura-2 or fura-6F as Ca^{2+} indicators. In some experiments, β cells were loaded by incubation with fura2-AM for 15 min at 37 °C in culture medium. Homogeneous $[Ca^{2+}]_i$ elevation was generated by photolysis of caged Ca^{2+} and DMN. Flashes of UV light and fluorescence-excitation light were generated as described (46). We used 5 mM DMN-containing internal solutions consisting of 110 mM CsCl, 5 mM DMN, 2 mM NaCl, 4.7 mM $CaCl_2$, 2 mM ATP, 0.3 mM GTP, 0.2 mM fura-6F and 35 mM HEPES. The basal $[Ca^{2+}]_i$ was measured to be approximately 200 nM by fura-2. Internal solutions were adjusted to pH 7.2 with either HCl or CsOH. $[Ca^{2+}]_i$ was calculated from the fluorescence ratio according to the equation: $[Ca^{2+}]_i = K_{eff} \times (R - R_{min})/(R_{max} - R)$, where K_{eff}, R_{min} and R_{max} are constants obtained from intracellular calibration as previously described (46). DMN, fura-2 and fura-6F were purchased from Molecular Probes (Eugene, OR, USA). Unless otherwise stated, all agents were purchased from Sigma (St.Louis, MO, USA).

Cm measurement

Conventional whole-cell recordings used sylgard-coated 2–3 MΩ pipettes. Series resistance ranging from 5 to 12 MΩ was included in the analysis. An EPC-9 patch-clamp amplifier was used together with PULSE + LOCK-IN software (HEKA Elektronics, Lambrecht, Germany). A 1042-Hz, 20-mV peak-to-peak sinusoidal voltage stimulus was superimposed on a holding potential of −70 mV. Currents were filtered at 2.9 kHz and sampled at 15 kHz.

To quantify the Ca^{2+} threshold for exocytosis, we obtained the rate of exocytosis from the derivative of Cm trace and fitted it with a polynomial function, from which we measure the $[Ca^{2+}]_i$ level at the half-maximal rate. To minimize the influence of the sustained component on the accurate determination of the RRP size, we fitted a straight line to the last slow phase of the Cm increase and extrapolated it back to the time when the half-maximal rate was reached. The difference (ΔCm) between this extrapolated level and the baseline Cm was our measure of RRP size (47, see also Figure 3).

Statistical analysis

The capacitance traces were imported to the IGOR Pro software (WaveMetrics, Lake Oswego, OR, USA), and the exocytotic burst were fitted with exponential function. Averaged results are presented as mean ± SEM. Statistical significance was evaluated using Student's *t*-test; $p < 0.05$ was considered to be statistically significant.

Acknowledgments

We thank Mrs X.P. Xu for skilled technical support in cell preparation. This work was supported by the National Science Foundation of China (Grants 30025023, 30270363 and 30130230), the National Basic Research Program of China (G1999054000 and 2004CB720000), the Knowledge Innovation Program (KSCX2-SW-224) and the Wellcome trust (GR074359MA, to Y.A.W). The laboratory of Tao Xu is also supported by the Partner Group Scheme of the Max Planck Institute for Biophysical Chemistry, Goettingen.

References

1. Frontali N, Ceccarelli B, Gorio A, Mauro A, Siekevitz P, Tzeng MC, Hurlbut WP. Purification from black widow spider venom of a protein factor causing the depletion of synaptic vesicles at neuromuscular junctions. J Cell Biol 1976;68:462–479.
2. Tzeng MC, Cohen RS, Siekevitz P. Release of neurotransmitters and depletion of synaptic vesicles in cerebral cortex slices by α-latrotoxin from black widow spider venom. Proc Natl Acad Sci USA 1978;75:4016–4020.
3. Petrenko AG, Kovalenko VA, Shamotienko OG, Surkova IN, Tarasyuk TA, Ushkaryov Y, Grishin EV. Isolation and properties of the α-latrotoxin receptor. EMBO J 1990;9:2023–2027.
4. Ushkaryov YA, Petrenko AG, Geppert M, Sudhof TC. Neurexins: synaptic cell surface proteins related to the α-latrotoxin receptor and laminin. Science 1992;257:50–56.
5. Krasnoperov VG, Beavis R, Chepurny OG, Little AR, Plotnikov AN, Petrenko AG. The calcium-independent receptor of α-latrotoxin is not a neurexin. Biochem Biophys Res Commun 1996;227:868–875.
6. Davletov BA, Shamotienko OG, Lelianova VG, Grishin EV, Ushkaryov YA. Isolation and biochemical characterization of a Ca^{2+}-independent α-latrotoxin-binding protein. J Biol Chem 1996;271:23239–23245.
7. Krasnoperov VG, Bittner MA, Beavis R, Kuang Y, Salnikow KV, Chepurny OG, Little AR, Plotnikov AN, Wu D, Holz RW, Petrenko AG. α-Latrotoxin stimulates exocytosis by the interaction with a neuronal G-protein-coupled receptor. Neuron 1997;18:925–937.
8. Lelianova VG, Davletov BA, Sterling A, Rahman MA, Grishin E, Totty NF, Ushkaryov Y. α-Latrotoxin receptor, latrophilin, is a novel member of the secretin family of G protein-coupled receptors. J Biol Chem 1997;272:21504–21508.
9. Krasnoperov V, Bittner MA, Mo W, Buryanovsky L, Neubert TA, Holz RW, Ichtchenko K, Petrenko AG. Protein-tyrosine phosphatase-σ is a novel member of the functional family of α-latrotoxin receptors. J Biol Chem 2002;277:35887–35895.
10. Tobaben S, Sudhof TC, Stahl B. Genetic analysis of α-latrotoxin receptors reveals functional interdependence of CIRL/latrophilin 1 and neurexin 1α. J Biol Chem 2002;277:6359–6365.
11. Grasso A, Alema S, Rufini S, Senni MI. Black widow spider toxin-induced calcium fluxes and transmitter release in a neurosecretory cell line. Nature 1980;283:774–776.
12. Orlova EV, Rahman MA, Gowen B, Volynski KE, Ashton AC, Manser C, van Heel M, Ushkaryov YA. Structure of α-latrotoxin oligomers reveals that divalent cation-dependent tetramers form membrane pores. Nat Struct Biol 2000;7:48–53.
13. Meldolesi J, Huttner WB, Tsien RY, Pozzan T. Free cytoplasmic Ca^{2+} and neurotransmitter release: studies on PC12 cells and synaptosomes exposed to α-latrotoxin. Proc Natl Acad Sci USA 1984;81:620–624.
14. Capogna M, Gahwiler BH, Thompson SM. Calcium-independent actions of α-latrotoxin on spontaneous and evoked synaptic transmission in the hippocampus. J Neurophysiol 1996;76:3149–3158.
15. Ashton AC, Rahman MA, Volynski KE, Manser C, Orlova EV, Matsushita H, Davletov BA, van Heel M, Grishin EV, Ushkaryov YA. Tetramerisation of α-latrotoxin by divalent cations is responsible for toxin-induced non-vesicular release and contributes to the Ca^{2+}-dependent vesicular exocytosis from synaptosomes. Biochimie 2000;82:453–468.
16. Capogna M, Volynski KE, Emptage NJ, Ushkaryov YA. The α-latrotoxin mutant LTX^{N4C} enhances spontaneous and evoked transmitter release in CA3 pyramidal neurons. J Neurosci 2003;23:4044–4053.
17. Ashton AC, Volynski KE, Lelianova VG, Orlova EV, Van Renterghem C, Canepari M, Seagar M, Ushkaryov YA. α-Latrotoxin, acting via two Ca^{2+}-dependent pathways, triggers exocytosis of two pools of synaptic vesicles. J Biol Chem 2001;276:44695–44703.
18. Ushkaryov YA, Volynski KE, Ashton AC. The multiple actions of black widow spider toxins and their selective use in neurosecretion studies. Toxicon 2004;43:527–542.
19. Khvotchev M, Sudhof TC. α-Latrotoxin triggers transmitter release via direct insertion into the presynaptic plasma membrane. EMBO J 2000;19:3250–3262.
20. Regazzi R, Wollheim CB, Lang J, Theler JM, Rossetto O, Montecucco C, Sadoul K, Weller U, Palmer M, Thorens B. VAMP-2 and cellubrevin are expressed in pancreatic β-cells and are essential for Ca^{2+} but not for GTPgS-induced insulin secretion. EMBO J 1995;14:2723–2730.
21. Xu T, Binz T, Niemann H, Neher E. Multiple kinetic components of exocytosis distinguished by neurotoxin sensitivity. Nat Neurosci 1998;1:192–200.
22. Lang J, Fukuda M, Zhang H, Mikoshiba K, Wollheim CB. The first C2 domain of synaptotagmin is required for exocytosis of insulin from pancreatic β-cells: action of synaptotagmin at low micromolar calcium. EMBO J 1997;16:5837–5846.
23. Lang J, Ushkaryov Y, Grasso A, Wollheim CB. Ca^{2+}-independent insulin exocytosis induced by α-latrotoxin requires latrophilin, a G protein-coupled receptor. EMBO J 1998;17:648–657.
24. Tse FW, Tse A. α-Latrotoxin stimulates inward current, rise in cytosolic calcium concentration, and exocytosis in pituitary gonadotropes. Endocrinology 1999;140:3025–3033.
25. Liu J, Misler S. α-Latrotoxin alters spontaneous and depolarization-evoked quantal release from rat adrenal chromaffin cells: evidence for multiple modes of action. J Neurosci 1998;18:6113–6125.
26. Ichtchenko K, Khvotchev M, Kiyatkin N, Simpson L, Sugita S, Sudhof TC. α-Latrotoxin action probed with recombinant toxin: receptors recruit α-latrotoxin but do not transduce an exocytotic signal. EMBO J 1998;17:6188–6199.
27. Volynski KE, Capogna M, Ashton AC, Thomson D, Orlova EV, Manser CF, Ribchester RR, Ushkaryov YA. Mutant α-latrotoxin (LTX^{N4C}) does not form pores and causes secretion by receptor stimulation: this action does not require neurexins. J Biol Chem 2003;278:31058–31066.
28. Xu T, Rammner B, Margittai M, Artalejo AR, Neher E, Jahn R. Inhibition of SNARE complex assembly differentially affects kinetic components of exocytosis. Cell 1999;99:713–722.
29. Wan QF, Dong Y, Yang H, Lou X, Ding J, Xu T. Protein kinase activation increases insulin secretion by sensitizing the secretory machinery to Ca^{2+}. J Gen Physiol 2004;124:653–662.
30. Davletov BA, Krasnoperov V, Hata Y, Petrenko AG, Sudhof TC. High affinity binding of α-latrotoxin to recombinant neurexin Ia. J Biol Chem 1995;270:23903–23905.
31. Sugita S, Khvochtev M, Sudhof TC. Neurexins are functional α-latrotoxin receptors. Neuron 1999;22:489–496.
32. Misler S, Falke LC. Dependence on multivalent cations of quantal release of transmitter induced by black widow spider venom. Am J Physiol 1987;253:C469–C476.
33. Brose N, Rosenmund C, Rettig J. Regulation of transmitter release by Unc-13 and its homologues. Curr Opin Neurobiol 2000;10:303–311.
34. Rhee JS, Betz A, Pyott S, Reim K, Varoqueaux F, Augustin I, Hesse D, Sudhof TC, Takahashi M, Rosenmund C, Brose N. β Phorbol ester- and diacylglycerol-induced augmentation of transmitter release is mediated by Munc13s and not by PKCs. Cell 2002;108:121–133.
35. Rosenthal L, Meldolesi J. α-Latrotoxin and related toxins. Pharmacol Ther 1989;42:115–134.
36. Sudhof TC. α-Latrotoxin and its receptors: neurexins CIRL/latrophilins. Annu Rev Neurosci 2001;24:933–962.
37. Wanke E, Ferroni A, Gattanini P, Meldolesi J. α-Latrotoxin of the black widow spider venom opens a small, non-closing cation channel. Biochem Biophys Res Commun 1986;134:320–325.

38. Van Renterghem C, Iborra C, Martin-Moutot N, Lelianova V, Ushkaryov Y, Seagar M. α-Latrotoxin forms calcium-permeable membrane pores via interactions with latrophilin or neurexin. Eur J Neurosci 2000;12:3953–3962.
39. Volynski KE, Meunier FA, Lelianova VG, Dudina EE, Volkova TM, Rahman MA, Manser C, Grishin EV, Dolly JO, Ashley RH, Ushkaryov YA. Latrophilin, neurexin, and their signaling-deficient mutants facilitate α-latrotoxin insertion into membranes but are not involved in pore formation. J Biol Chem 2000;275:41175–41183.
40. McMahon HT, Rosenthal L, Meldolesi J, Nicholls DG. α-Latrotoxin releases both vesicular and cytoplasmic glutamate from isolated nerve terminals. J Neurochem 1990;55:2039–2047.
41. Rahman MA, Ashton AC, Meunier FA, Davletov BA, Dolly JO, Ushkaryov YA. Norepinephrine exocytosis stimulated by α-latrotoxin requires both external and stored Ca^{2+} and is mediated by latrophilin, G proteins and phospholipase C. Philos Trans R Soc Lond B Biol Sci 1999;354:379–386.
42. Yang Y, Gillis KD. A highly Ca^{2+}-sensitive pool of granules is regulated by glucose and protein kinases in insulin-secreting INS-1 cells. J Gen Physiol 2004;124:641–651.
43. Bittner MA, Holz RW. Latrotoxin stimulates secretion in permeabilized cells by regulating an intracellular Ca^{2+}- and ATP-dependent Event. J Biol Chem 2000;275:25351–25357.
44. Lou XL, Yu X, Chen XK, Duan KL, He LM, Qu AL, Xu T, Zhou Z. Na^{+} channel inactivation: a comparative study between pancreatic islet β-cells and adrenal chromaffin cells in rat. J Physiol 2003;548:191–202.
45. Rorsman P, Trube G. Calcium and delayed potassium currents in mouse pancreatic β-cells under voltage-clamp conditions. J Physiol 1986;374:531–550.
46. Xu T, Naraghi M, Kang H, Neher E. Kinetic studies of Ca^{2+} binding and Ca^{2+} clearance in the cytosol of adrenal chromaffin cells. Biophys J 1997;73:532–545.
47. Zhu H, Hille B, Xu T. Sensitization of regulated exocytosis by protein kinase C. Proc Natl Acad Sci USA 2002;99:17055–17059.